Hematological Oncology
Hematol Oncol 2008; **26**: 199–211
Published online 6 May 2008 in Wiley InterScience
(www.interscience.wiley.com) **DOI**: 10.1002/hon.859

Research Article

Genetic and phenotypic analysis of B-cell post-transplant lymphoproliferative disorders provides insights into disease biology

Efsevia Vakiani[1], Katia Basso[2], Ulf Klein[2], Mahesh M. Mansukhani[1], Gopeshwar Narayan[2], Paula M. Smith[2], Vundavalli V. Murty[1,2], Riccardo Dalla-Favera[1,2], Laura Pasqualucci[1,2] and Govind Bhagat[1]*

[1]*Department of Pathology, Columbia University, New York, NY 10032, USA*
[2]*Institute for Cancer Genetics, Columbia University, New York, NY 10032, USA*

**Correspondence to:*
Dr Govind Bhagat, Department of Pathology, College of Physicians and Surgeons, Columbia University, VC14-228, 630W 168th street, New York, NY 10032, USA.
E-mail: gb96@columbia.edu

Received: 3 February 2008
Revised: 16 March 2008
Accepted: 27 March 2008

Abstract

B-cell post-transplant lymphoproliferative disorders (PTLD) are classified as early lesions, polymorphic lymphomas (P-PTLD) and monomorphic lymphomas (M-PTLD). These morphologic categories are thought to reflect a biologic continuum, although supporting genetic data are lacking. To gain better insights into PTLD pathogenesis, we characterized the phenotypes, immunoglobulin (Ig) gene alterations and non-Ig gene (*BCL6*, *RhoH/TTF*, *c-MYC*, *PAX5*, *CIITA*, *BCL7A*, *PIM1*) mutations of 21 PTLD, including an IM-like lesion, 8 P-PTLD and 12 M-PTLD. Gene expression profile analysis was also performed in 12 cases. All PTLD with clonal Ig rearrangements showed evidence of germinal centre (GC) transit based on the analysis of Ig and *BCL6* gene mutations, and 74% had a non-GC phenotype (BCL6 ± MUM1+). Although surface Ig abnormalities were seen in 6/19 (32%) PTLD, only three showed 'crippling' Ig mutations indicating other etiologies for loss of the B-cell receptor. Aberrant somatic hypermutation (ASHM) was almost exclusively observed in M-PTLD (8/12 vs. 1/8 P-PTLD) and all three recurrent cases analysed showed additional mutations in genes targeted by ASHM. Gene expression analysis showed distinct clustering of PTLD compared to B-cell non-Hodgkin lymphomas (B-NHL) without segregation of P-PTLD from non-GC M-PTLD or EBV+ from EBV− PTLD. The gene expression pattern of PTLD appeared more related to that of memory and activated B-cells. Together, our results suggest that PTLD represent a distinct type of B-NHL deriving from an antigen experienced B-cell, whose evolution is associated with accrual of genetic lesions.

Keywords: post-transplant lymphoproliferative disorder; gene expression profile; aberrant somatic hypermutation; phenotype

Introduction

Post-transplant lymphoproliferative disorders (PTLD) encompass a heterogeneous group of lymphocytic proliferations, the vast majority of which are of B-cell origin. The current WHO classification categorizes them as early lesions, polymorphic lymphomas (P-PTLD) and monomorphic lymphomas (M-PTLD). Virtually, all early lesions are polyclonal and they appear to lack any known molecular alterations [1]. Many P-PTLD and most M-PTLD are clonal [1,2]. Compared to P-PTLD, M-PTLD harbour more karyotypic abnormalities, have a higher frequency of alterations of protooncogenes and carry mutations in a number of tumour-suppressor genes [1,3,4]. Mutations in genes due to aberrant somatic hypermutation (ASHM), a recently identified B-cell specific mechanism of genetic instability, have been reported to occur exclusively in M-PTLD [5,6]. The presence of distinct as well as shared cytogenetic aberrations among P-PTLD and M-PTLD [4] suggests that certain M-PTLD might arise as independent primary neoplasms, while others may represent progression of P-PTLD. The relationship of P-PTLD to M-PTLD, however, remains unknown.

Our understanding of the cellular origin of PTLD also remains unclear. A limited number of studies have shown that the vast majority of cases bear an imprint of germinal centre (GC) transit, as evidenced by the presence of somatically mutated immunoglobulin (Ig) genes, and most have non-GC immunophenotypes (BCL6 ± MUM1+) [2,7,8]. However, more sensitive approaches, such as gene expression profiling, which have significantly advanced our knowledge of B-cell non-Hodgkin lymphoma (B-NHL) biology, have not been systematically applied to the study of PTLD.

The pathogenesis of PTLD is commonly associated with Epstein–Barr virus (EBV) infection, although in more recent studies 23–42% of PTLD have been reported to be EBV− [2,9]. It has been proposed that EBV− PTLD may be similar to B-NHL of immunocompetent hosts [10]; yet, a number of them respond to decreased immunosuppression, suggesting that immune deregulation plays a role in

the pathogenesis of at least a subset of EBV− PTLD [9]. A minority of PTLD also lack surface B-cell receptor (BCR) and it is speculated that EBV-encoded proteins can substitute for BCR signalling and survival of the abnormal clones [11]. The relationship of EBV− PTLD to EBV+ PTLD or B-NHL occurring in immunocompetent individuals is not known at present.

To gain better insights into the pathogenesis of PTLD, we performed comprehensive phenotypic and genetic characterization of 21 PTLD. Gene expression profiles of a subset of cases were also analysed and compared to other types of B-NHL and cells representing normal B-cell maturational stages.

Materials and methods

Case selection and morphologic analysis

We searched our departmental database to identify PTLD for which frozen tissue samples were available. Frozen sections were reviewed prior to and after obtaining tissue for molecular studies, to assess tumour content and ensure morphologic representation, and only cases with >90% lesional composition were used. Sections of formalin-fixed, paraffin-embedded tissue from the corresponding cases were stained with haematoxylin and eosin for morphologic review. PTLD were classified according to the current WHO criteria [12]. This study was approved by the Institutional Review Board of Columbia University.

Immunohistochemistry, *in situ* hybridization and flow cytometry

Immunohistochemical (IHC) stains were performed on paraffin-embedded tissue sections after moist heat-induced antigen retrieval, using an autostainer (Universal staining system, DAKO, Carpinteria, CA) and the primary antibodies listed in Table 2. The Envision Plus kit (DAKO) was used for detection. Staining for BLIMP-1 and activation-induced deaminase (AID) was performed as previously described [13,14].

Cases were scored as positive if >20% cells expressed the analysed antigen, except for LMP1, EBNA2 and BZLF1, where percentage of cellular expression was recorded.

In situ hybridization for EBV-encoded small RNAs (EBER) was performed using the manufacturer's protocol (INFORM EBER, Ventana, Tucson, AZ).

Three or four colour flow cytometric analysis (FACScan; BD Biosciences, San Diego, CA) was performed using a comprehensive panel of antibodies against B- and T-cell antigens, including Ig light (Ig_L) and heavy chains (Ig_H), according to standard methods. Data were analysed using the Cell Quest software (BD Biosciences).

DNA and RNA extraction

Genomic DNA and total RNA were extracted from frozen tissue according to standard methods. In all PTLD and in selected matched non-neoplastic tissue specimens, DNA was also extracted from paraffin-embedded tissue using the QIAamp DNA mini Kit (QIAGEN, Valencia, CA).

Analysis of IgV_H genes

PCR amplification of the Ig heavy chain variable region (V_H) genes was performed using DNA extracted from frozen tissue initially with IgV_H gene family specific (V_H1–6) primers that hybridize to framework region (FR) 1 sequences and an antisense J_H primer mix. If no clonal IgV_H gene rearrangement was obtained, DNA was amplified with V_H1,3,4 primers that hybridize to the IgV_H leader (L) region (sequences for all primers have been previously reported [15,16]). PCR products were purified and sequenced as described [17], and sequences were compared to the most homologous germline V_H genes in the IMGT (https://imgt.cines.fr) and IgBLAST (http://www.ncbi.nlm.nih.gov/igblast/) databases. The presence of IgV_H rearrangements was also determined using FR3 primers and DNA extracted from paraffin-embedded tissue as previously described [18].

The ratio of replacement to silent mutations in the complementarity determining regions and FRs was analysed using the multinomial distribution model available at www-stat.stanford.edu/immunoglobulin [19]. Determination of antigen selection was based on the analysis of FR mutations since interpretation of complementarity determining region mutations is controversial [20].

Analysis of *BCL6*, *PIM1*, *PAX5*, *RhoH/TTF*, *c-MYC*, *CIITA* and *BCL7A*

The oligonucleotide sequences used for amplification of the *BCL6*, *PIM1*, *PAX5*, *RhoH/TTF*, *c-MYC*, *CIITA* and *BCL7A* 5′ sequences and the genomic regions amplified are described in Supplemental Table 1. These regions correspond to the intervals previously shown to harbour >95% of all *BCL6* mutations detected in B-NHL [21] and >90% of mutations affecting the remaining six genes in diffuse large B-cell lymphomas (DLBCL) [6] (L. P., unpublished data). Purified amplicons were sequenced directly as described [17] and compared to the corresponding germline sequences (Supplemental Table 1) as previously reported [6]. Nucleotide changes due to previously reported polymorphisms or present in paired normal DNA (where available) were excluded from the calculation of mutation frequencies [6].

Generation of gene expression profiles and data analyses

Gene expression profile analysis was performed on 12 PTLD (1 IM-like lesion, 5 P-PTLD and 6 M-PTLD). A case each of IM-like lesion and M-PTLD of GC phenotype were included for analysis; the former, since cellular composition of the interfollicular areas in such lesions is morphologically indistinguishable from P-PTLD, and the latter, to determine any overriding effect of the post-transplant status (effect of immunosuppressive medi-

DOI: 10.1002/hon

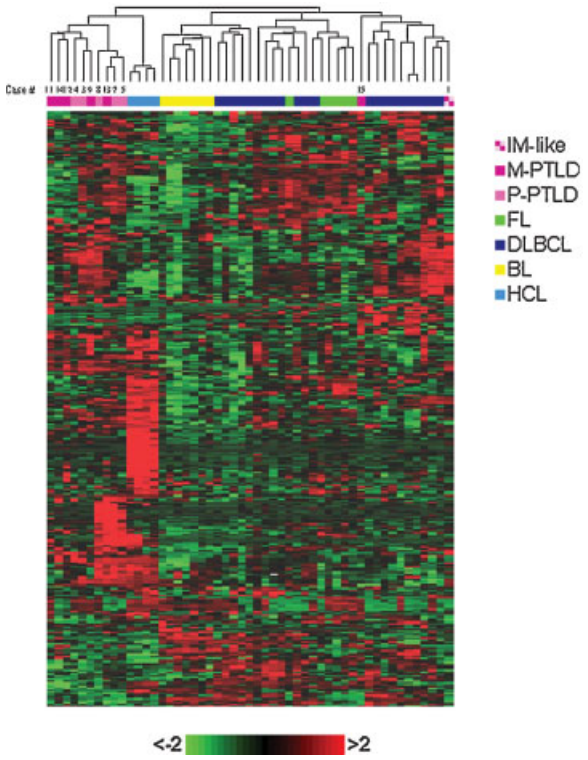

Figure 1. Unsupervised hierarchical clustering performed on a representative panel of B-NHL, including 22 diffuse large B-cell lymphomas (DLBCL), 6 follicular lymphomas (FL), 7 Burkitt lymphomas (BL), 4 hairy cell leukaemias (HCL) and 12 PTLD; 5 polymorphic (P-PTLD), 6 monomorphic (M-PTLD) and 1 IM-like lesion (case numbers shown correspond to PTLD in Table 1). Clustering is based on the expression of 333 genes. (Colour scale identifies relative gene expression changes normalized by the standard deviation—zero representing the mean expression level of a given gene across the panel)

cations on the lymphoproliferations or their microenvironment) on the pattern of segregation of PTLD. Suboptimal RNA quality and insufficient numbers of distinct morphologic types of M-PTLD (e.g. BL) precluded analysis of the remaining cases. Complementary RNA was prepared as previously described and hybridized to HG-U95Av2 microarrays (Affymetrix, Santa Clara, CA) [22]. Gene expression values were determined by the GCOS 1.4 Microarray Suite 5.0 software (Affymetrix) using the Global Scaling option. In conjunction with previously generated expression profile data of other B-NHL subsets (derived from B-cells at different maturational stages), including EBV− DLBCL ($n = 22$; 14 centroblastic and 8 immunoblastic), follicular lymphoma (FL, $n = 6$), Burkitt lymphoma (BL, $n = 7$; 1 EBV+ and 6 EBV−), and hairy cell leukaemia (HCL, $n = 4$) [23,24], a hierarchical clustering algorithm based on the average-linkage method was used to generate the dendrogram in Figure 1 [25]. Expression values of the selected genes were normalized to have a zero mean value and unit standard deviation, and the distance between two individual samples was calculated by Pearson distance analysis.

Supervised analysis was performed using the Genes@-Work software platform [26]. PTLD gene expression profiles were compared to mantle cell lymphoma (MCL, $n = 7$), HCL ($n = 8$), chronic lymphocytic leukaemia (CLL, $n = 10$), FL ($n = 6$), BL ($n = 7$), DLBCL, including centroblastic ($n = 15$) and immunoblastic ($n = 8$) subtypes, and purified normal B-cell subsets (5 naïve, 5 memory and 10 GC) [17,23,27]. Cell type classification was performed as previously described [27]. Briefly, the classifier is a scoring function based on a set of differentially expressed genes between two phenotypes (higher score implies closer relatedness of the test sample to the phenotype set).

Statistical analysis

Fisher's exact test and Student's *t*-test were performed to evaluate differences between datasets consisting of categorical and numerical variables, respectively, and a p-value < 0.05 was considered significant. Where applicable, the Spearman's rank correlation coefficient was also evaluated.

Results

Patient characteristics

Twenty-one PTLD from 18 patients (10M, 8F), including 3 recurrent PTLD, were studied (Table 1). Seven patients presented with nodal and 11 with extranodal disease. Median age at initial diagnosis was 21 years (mean 27.5 years, range 2–64 years) and the median time from transplant to initial diagnosis was 7.5 years (mean 6.0 years, range 0.3–17 years). P-PTLD occurred significantly earlier than M-PTLD (3.1 vs. 8.7 years, $p = 0.02$). Six patients are currently alive 1.7–5 years (median 2.6 years, mean 2.8 years) following initial presentation and 11 patients died 1 month–16 years (median 1.2 years, mean 2.9 years) post-diagnosis, 6 of PTLD and 5 of other causes. All three patients whose recurrent PTLD were analysed had variable durations of remissions between recurrences (1.2, 1.7 and 14 years).

Morphologic and phenotypic analysis

PTLD cases were classified as IM-like lesion ($n = 1$), P-PTLD ($n = 8$) and M-PTLD ($n = 12$). M-PTLD were further classified as DLBCL ($n = 10$) and BL ($n = 2$); the DLBCL were predominantly composed of centroblast-like cells. Morphologic features of the 12 PTLD used for gene expression profiling are shown in Supplemental Figure 1.

The results of IHC staining are shown in Table 2. The neoplastic cells in all 7 P-PTLD tested and in 7/10 (70%) DLBCL were CD10-/BCL6±/MUM1+/CD138−; these cases were classified as having a non-GC (post-GC) phenotype (Table 1) [28]. Three of 10 (30%) DLBCL and both BL had a GC phenotype (CD10±/BCL6+/MUM1−/CD138−). Neoplastic cells in all PTLD expressed PAX5 and CD79a, and all except one were OCT2+; diminished ($n = 4$) or absent ($n = 1$) CD20 expression was seen in five cases (2/7, 29% P-PTLD, 3/12, 25% M-PTLD) by IHC staining and flow cytometry. One OCT2 + DLBCL lacked OCT2 expression on recurrence. One of 7 (14%) P-PTLD and 9/12 (75%) M-PTLD ($p = 0.02$) expressed PU.1.

DOI: 10.1002/hon

Table 1. Clinical and pathologic characteristics of patients with PTLD

Case	Age at dx (years)	Sex	Tx organ	PTLD type	IHC phenotype	EBV*	EBV latency	Surface light chain	Surface heavy chain	Site	Time since tx (years)	Immuno-Rx	Treatment	Outcome (time)
1†	9	F	Heart	IM-like lesion	NA	+	I	Polyclonal	IgM, IgD	Tonsil	9	C, P	No treatment	D‡ (14 months)
2	2	F	Heart	P-PTLD	Non-GC	+	III	Absent	ND	Tonsil	1.5	FK506	DI	D§ (4 months)
3	23	M	Heart	P-PTLD	Non-GC	–	NA	Polyclonal‖	ND	Lymph node	12	C	DI, CT	A (5 years)
4	21	M	Kidney	P-PTLD	Non-GC	+	II	Absent	ND	Lymph node	8	C, A, P	Rituxan, CT	D (4 month)
5	56	F	Lung	P-PTLD	Non-GC	+	III	Kappa	ND	Lymph node	0.3	FK506, A, P	RT, rituxan	D (5 month)
6	21	M	Kidney	P-PTLD	Non-GC	+	III	Polyclonal	IgM, IgD	Lymph node	0.5	FK506, M, P	DI, CT, rituxan	D§ (1.2 years)
7	2.5	F	Heart	P-PTLD	Non-GC	+	III	Polyclonal	ND	Tonsil	0.8	FK506, A	DI	A (2.3 years)
8	6	F	Heart	P-PTLD	Non-GC	–	NA	Absent¶	IgM	Tonsil	1	C, M, P	DI, RT	A (2.5 years)
9	60	M	Kidney	M-PTLD	Non-GC	+	III	Polyclonal‖	ND	Soft tissue	8	C, P	DI, rituxan	D# (3 years)
10a	64	M	Kidney	M-PTLD	GC	–	NA	Absent	ND	Lymph node	3.3	FK506, M, P	CT, rituxan	D** (2 years)
10b	65			M-PTLD	GC			Absent	absent	Pleural fluid	4.5			
11	39	M	Heart	M-PTLD	Non-GC	–	NA	Polyclonal‖	ND	Small intestine	8	C, P	CT, rituxan	D (3 month)
12	11	F	Liver	M-PTLD	Non-GC	+	III	Diminished††	IgG	Lymph node	7	FK506, P	DI, CT	D (1 month)
13	18	F	Kidney	M-PTLD	Non-GC	+	III	Polyclonal	ND	Tonsil	0.8	FK506, M, P	CT, rituxan	D‡‡ (6.7 years)
14a	11	F	Heart	M-PTLD	Non-GC	+	II	Kappa	IgA	Small intestine	10	FK506, A, P	DI, RT, CT	A** (2.6 years)
14b	13			M-PTLD	Non-GC	–	NA	Kappa	IgA	Lung	11.7			
15	51	M	Kidney	M-PTLD	GC	–	NA	Kappa	ND	Lymph node	17	C, A, P	RT	LTF
16a	61	M	Heart	P-PTLD	ND	–	NA	ND	ND	Lung	1	C, M, P	CT	D** (16 years)
16b	75			M-PTLD	Non-GC			Kappa	ND	Lymph node	15		CT	
17	25	M	Kidney	M-PTLD	GC	–	NA	Lambda	IgM	Colon	8	FK506, M, P	CT	A (2.6 years)
18	15	M	Heart	M-PTLD	GC	+	I	ND	ND	Retroperitoneum	11	C, M	CT	A (1.7 years)

IM, infectious mononucleosis; P-PTLD, polymorphic post-transplant lymphoproliferative disorder; M-PTLD, monomorphic PTLD; GC, germinal centre; BL, Burkitt lymphoma; Immuno-Rx, immunosuppression; tx, transplant; dx, diagnosis; C, cyclosporine; P, prednisone; A, azathioprine; M, mycophenolate; DI, decreased immunosuppression; CT, chemotherapy; RT, radiation; D, dead; A, alive; LTF, lost to follow up; ND, not done; NA, not applicable.

*Based on EBER *in situ* hybridization.

†Cases in bold were also used for gene expression profiling.

‡Died from rejection related heart failure.

§Died from sepsis.

‖Gated population of B-cells was small (2–12%).

¶Cytoplasmic lambda expression was seen.

#Died from gastric cancer.

**Time from initial diagnosis.

††Cytoplasmic kappa expression was seen.

‡‡Died from papillary serous carcinoma.

DOI: 10.1002/hon

PTLD with a non-GC phenotype showed weak PU.1 staining, in contrast to PTLD with a GC phenotype (moderate to strong PU.1 staining), suggesting a correlation of PU.1 expression with GC phenotype, similar to DLBCL of immunocompetent individuals [29]. Neoplastic cells of 3/12 (25%) M-PTLD expressed BLIMP-1, while only plasma cells expressed BLIMP-1 in P-PTLD. One DLBCL that was HLA-DR− by IHC (and dim HLA-DR+ by flow cytometry) had an aggressive course similar to that reported for HLA-DR− DLBCL of immunocompetent hosts [30]. Cytoplasmic staining for AID, an enzyme required for SHM and class switch recombination [31], was seen only in M-PTLD (0/7 vs. 10/12, $p < 0.005$). Only a minority of nuclei in each case (rare—5%) showed AID expression. There was no evidence of human herpes virus 8 infection as assessed with a stain for latency-associated nuclear antigen (LANA).

Flow cytometric assessment of Ig_L and surface Ig_H (sIg_H) expression performed in 19 and 8 PTLD, respectively, demonstrated Ig_L restriction in 8/19 (42%) PTLD. A dominant sIg_H was detected in 5/8 (63%) PTLD. Absent or diminished sIg_L expression was seen in 6/19 (32%) PTLD (3 P-PTLD, 3 M-PTLD); however, monotypic cytoplasmic light chains and sIg_H were detected in 2 of these cases (Table 1).

EBV infection

Evidence of EBV infection (EBER+) was found in 11/21 (52%) samples, including the IM-like lesion, 5/8 (63%) P-PTLD, and 5/12 (42%) M-PTLD (4/10 DLBCL, 1/2 BL). One EBER+ (and OCT2+) M-PTLD was EBER− (and OCT2−) on recurrence 1.7 years later. The types of viral latency are shown in Table 1. The IM-like lesion showed only rare (up to 5/HPF) scattered EBER+/LMP1−/EBNA2− cells (latency I), while 4/5 (80%) P-PTLD and 3/5 (60%) M-PTLD exhibited latency type-III infection (LMP1+/EBNA2+). The number of LMP1+ and EBNA2+ cells, however, varied significantly, indicating heterogeneity in latency types within a given PTLD, as shown previously [32]. One case each of a P-PTLD and M-PTLD had latency type-II (LMP-1+/EBNA2−) and the EBER+ BL had latency type-I infection. All 5 EBV+ P-PTLD and 2/5 (40%) EBV+ M-PTLD showed variable BZLF1 (lytic phase protein) expression, similar to previous reports (Table 2) [32].

The majority of non-GC PTLD were EBV+ (9/14) and the majority of GC PTLD were EBV− (4/5); however, the correlation between phenotype and EBV infection did not reach statistical significance ($p = 0.14$). There was no significant difference in the mean time from transplant to initial presentation between EBV+ and EBV− PTLD (5.2 vs. 7.2 years, $p = 0.42$). AID expression was observed more frequently in EBV− PTLD, although the difference was not statistically significant (7/9 vs. 3/10, $p = 0.07$).

Analysis of IgV_H rearrangements and mutations

Clonal IgV_H gene rearrangements were detected in the majority of PTLD (16/21, 76%) and all except one harboured somatic mutations (mean frequency 9.2%, range 3.7–19.3%) (Table 3, Supplemental Table 2). The case lacking IgV_H gene mutations had mutations in *BCL6* (case #7, Table 3). Overall, these findings indicate an origin of PTLD from GC experienced B-cells. There was no significant difference in the average IgV_H mutation frequency between P-PTLD (7.7%) and M-PTLD (10.3%, $p = 0.38$) or between EBV− PTLD (10.6%) and EBV+ PTLD (7.5%, $p = 0.26$).

Potentially functional Ig genes were predicted in 13 (81%) of the 16 clonally rearranged PTLD (5/6 P-PTLD and 8/10 M-PTLD, Supplemental Table 2). The remaining three (19%) cases displayed an original in-frame rearrangement that had acquired crippling mutations: one of these, an EBV+ P-PTLD, had a 295 (bp) deletion involving FR1 and FR2; two other samples, representing clonally related EBV− M-PTLD from the same patient, had a 1 bp deletion in the FR3 region, resulting in a frameshift with premature stop codon. All these three cases showed absent sIg_L expression (and sIg_H in one case evaluated) by flow cytometry. Notably, virtually all mutated functional rearrangements (11/12) showed lower than expected number of replacement FR mutations, indicating selection due to antigen pressure.

Analysis of *BCL6* mutations

In agreement with previous studies, *BCL6* mutations were seen in 14/21 (67%) PTLD (Table 3) [2,3]. A total of 46 independent mutations were detected (mutations in >1 sample from the same patient were counted once), corresponding to an average mutation frequency of 0.11/100 bp in the mutated cases (range, 0.06–0.45/100 bp). Of these, the majority were represented by single bp substitutions ($n = 43$, 18 transitions, 25 transversions, ratio 0.72) and three were deletions.

No significant differences were observed between P-PTLD and M-PTLD with respect to total number of cases carrying *BCL6* mutations (5/8, 63% vs. 9/12, 75%, $p = 0.6$) and average mutation frequency (0.12/100 bp vs. 0.35/100 bp, $p = 0.19$). The presence (or frequency) of *BCL6* mutations also did not correlate with the type of organ transplanted, immunosuppression, site of PTLD (nodal vs. extranodal), phenotype, EBV infection or AID expression. Contrary to a prior study [3], the presence of *BCL6* mutations showed no correlation with clinical outcome. However, patients who died from disease had a significantly higher mutation frequency compared to those who are alive or died from other causes (0.32/100 bp vs. 0.05/100 bp, $p = 0.03$).

Analysis of genes targeted by ASHM

To examine the role of ASHM in the pathogenesis and progression of PTLD, we sequenced the 5′ region of six non-Ig genes previously identified as ASHM targets, including two (*CIITA* and *BCL7A*) that have not been previously reported (L. P., unpublished observation). No mutations were seen in the IM-like lesion and this case was excluded from further analysis, since a clonal population

DOI: 10.1002/hon

Table 2. Immunohistochemical staining profiles of PTLD

Antibody	Clone, dilution company	IM-like lesion*	P-PTLD							M-PTLD, DLBCL									M-PTLD, BL	
		1	2	**3**	**4**	**5**	6	**7**	**8**	**9**	10a,b	**11**	**12**	**13**	**14a**	14b	**15**	16b	17	18
PAX5	SER 393, ND Cell Marque	+	+	+	+	+	+	+	+	+	+	+	+	+	+	+	+	+	+	+
CD79a	JCB117, 1:500 DAKO	+	+	+	+	+	+	+	+	+	+	+	+	+	+	+	+	+	+	+
CD20	L26, 1:1000 DAKO	+	Dim	+	+	+	+	+	Dim	+	+	+	−	+	Dim	Dim	+	+	+	+
CD10	CALLA, 1:30 Novocastra	+ (GC)	−	−	−	−	−	−	−	−	+	−	−	−	−	−	−	+	+	+
BCL6	PG-B6P, 1:40 DAKO	+ (GC)	−	−	−	−	−	−	−	−	+	−	−	−	−	−	+	+	+	+
MUM1	MUM1P, 1:50 DAKO	+	+	+	+	+	+	+	+	+	−	+	+	+	+	+	−	+	+	+
BLIMP-1†	63, 1:100 Santa Cruz	+	−	−	−	−	−	−	−	−	−	−	70%	−	20%	20%	−	−	−	−
CD138	M7228, 1:80 DAKO	+	−	−	−	−	−	−	−	−	−	−	−	−	−	−	−	−	−	−
OCT2	E978, 1:400 Santa Cruz	+	+	+	+	+	+	+	+	+	+	+	+	+	+	−	+	+	+	+
PU.1	G148–74, 1:40 BD Biosciences	+	−	−	−	+ (w)	−	−	−	+ (w)	+	+	−	+ (w)	−	−	+	+ (w)	+	+
HLA-DR	LN3, 1:150 Biogenex	+	+	+	+	+	+	+	+	+	+	+	−	+	+	+	+	+	+	+
LMP1‡	CSI-4, 1:200 DAKO	−	10%	NA	25%	50%	80%	30%	NA	60%	NA	NA	30%	70%	10%	NA	NA	NA	NA	−
EBNA2‡	PE2,1:100 DAKO	−	10%	NA	−	50%	80%	30%	NA	60%	NA	NA	50%	70%	−	NA	NA	NA	NA	−
BZLF1‡	BZ-1, 1:40 DAKO	−	5%	NA	5%	5%	5%	5%	NA	−	NA	NA	20%	−	10%	NA	NA	NA	NA	−
LANA	13B10, 1:100 Cell Marque	−	−	−	−	−	−	−	−	−	−	−	−	−	−	−	−	−	−	−
AID	EK2 5G9, 1:100 Cell Signalling	+	−	−	−	−	−	−	−	−	20%	70%	20%	−	30%	30%	30%	40%	90%	80%

IM, infectious mononucleosis; P-PTLD, polymorphic post-transplant lymphoproliferative disorder; M-PTLD, monomorphic PTLD; DLBCL, diffuse large B-cell lymphoma; GC, germinal centre; BL, Burkitt lymphoma; w, weak staining; dim, diminished; NA, not applicable; ND, not diluted.

*Unless specified as expression in GC cells, the results denote presence of populations of B-cells in the interfollicular area with expression of these antigens; AID staining was present both in GC cells and in extrafollicular blasts.

†Staining results shown for neoplastic cells; plasma cells were positive in all P-PTLD.

‡Expressed as percentage of EBER positive cells.

DOI: 10.1002/hon

Table 3. Analyses of IgV_H, *BCL-6*, *PIM1*, *PAX-5*, *Rhoh/TTF*, *c-MYC*, *BCL7A* and *CIITA* mutations in PTLD

Case	Histology	IgV_H gene analysis*		Mutations (position)							
		V_H family (gene)	Mutation frequency (%)	*BCL6*	*PIM1*	*PAX5*	*RhoH/TTF*	*c-MYC*	*BCL7A*	*CIITA*	Outcome
1†	IM-like lesion	NA	na	–	–	–	–	–	–	–	DOC
2	P-PTLD	NA	na	–	–	–	–‡	–	–	–	DOC
3	P-PTLD	V1–69	19.3	C435G	–	–	–	–	–	–	NED
4	P-PTLD	V4–39	3.7	A511G, A542G, A559G, del671A	–	–	–	–	–	–	DOD
5	P-PTLD	V1–8	11.6	C476G	–	–	–	–	–	–	DOD
6	P-PTLD	V3–23	7.8	–	–	–	–	–	–	–‡	DOC
7	P-PTLD	V3–33	0	C445G§, A493C§	–	–	–	–	–	–	NED
16a	P-PTLD	NA	na	T647A, T729G	–	–	G555C§	–‖	–	–	DOD
8	P-PTLD	V4–30	3.8	–	–	–	–	–‡	–	–	NED
9	M-PTLD, DLBCL	V3–30	8.2	G688C, T869G, C904A	–	–	–	–	–	–	DOC
10a	M-PTLD, DLBCL	V3–33	16.2	T606G, del609C, C776G, C780G, C789G, G798A, C806T, C864G, C935T, C958G, C1048G, G1057A, C1084G, T1099G, G1136A¶	–	–	–	–	–	907C-T, 1292C-A, 1363G-A, 1367G-A, 1415G-A, 1416G-A	DOD
10b	M-PTLD, DLBCL	V3–33	16.9	T606G, del609C, C776G, C780G, C789G, G798A, C806T, C864G, C864T, C935T, C958G, C1048G, G1057A, C1084G, T1099G, G1136A¶	–	–	–	del17bp (2974–2990)	dup21bp (618–638)	907C-T, 1292C-A, 1363G-A, 1367G-A, 1415G-A, 1416G-A	
11	M-PTLD, DLBCL	V4–34	7.8	–	–	–	–	–	–	del1358G	DOD
12	M-PTLD, DLBCL	NA	na	A639T, T777G, T793C, del3bp (795–797), C832T, T869G, G1066A	–	–	A625C§	–	–	–	DOD
13	M-PTLD, DLBCL	V3–23	13.1	–	–	–	–	–	–	–	DOC
14	M-PTLD, DLBCL	V3–48	5.6	C480T§	–	–	–	C2572T§	–	–	AWD
14b	M-PTLD, DLBCL	V3–48	5.6	C480T	–	–	–	C2572T, del2841C, G2983A	–	–	
15	M-PTLD, DLBCL	V4–39	13.4	T464C, T470C, T606C, T703C, T777G, G794T, A862G	–	–	–	–	–	–	LTF
16b	M-PTLD, DLBCL	NA	na	T647A, T729G	–	C1334T, G1435A	G555C, A619G, A672G	C2687T	G158A, G379C, A398C	G1091A	DOD
17	M-PTLD, BL	V3–7	8	–	–	–	–	G4450C, G5226A#	–	–	NED
18	M-PTLD, BL	V3–30	10.1	C751A, C883G	–	–	A376C, A460C	G2408C, T2504C, G2654A, A2711G,C2734G, G2739A, C2838T, T2846G, G2851A, G2933A, A2954C#	–	–	NED

IM, infectious mononucleosis; P-PTLD, polymorphic post-transplant lymphoproliferative disorder; M-PTLD, monomorphic PTLD; DLBCL, diffuse large B-cell lymphomas; BL, Burkitt lymphoma; NA, not amplified; na, not applicable; del, deletion; dup, duplication; –, wildtype sequence; DOC, dead from other causes; DOD, dead of disease; NED, no evidence of disease; AWD, alive with disease; LTF, lost to follow-up.

*Only in-frame rearrangements are listed.

†Cases in bold were also used for gene expression profiling.

‡Analysis of the corresponding germline DNA led to the reassignment of three putative mutations as polymorphisms; 927A-G (RhoH/TTF), 5028G-A (c-MYC) and 982G-A (CIITA).

§Confirmed by sequencing normal DNA.

‖Only exon 2 amplified.

¶The high number of *BCL6* mutations most likely resulted from a translocation t(2;3)(p11.2;q27) that juxtaposed *BCL6* to the Ig kappa gene promoter (2p11.2).

#*c-MYC* mutations in both BL were excluded from the analysis because these cases carry a t(8;14) translocation and the mutations were attributed to the juxtaposed Ig elements.

DOI: 10.1002/hon

was not detected. Mutations affecting at least one gene were found in 9/20 (45%) PTLD samples from six patients (Table 3). *PAX5* was mutated in 1/20 (5%), *RhoH/TTF* in 4/20 (20%), *c-MYC* in 4/18 (22%), *BCL7A* in 2/20 (10%) and *CIITA* in 4/20 (20%) PTLD. No *PIM1* mutations were observed. In total, 25 independent mutations were seen, consisting of 21 single bp substitutions (13 transitions, 8 transversions, ratio 1.63), three deletions and one duplication.

ASHM was significantly more frequent in M-PTLD than in P-PTLD (8/12 vs. 1/8 mutated cases, $p = 0.028$), and correlated with AID expression (8/10 vs. 0/9, $p < 0.005$). When considering EBV status, ASHM was observed more frequently in EBV− PTLD, both with regard to total number of cases (6/10 vs. 3/10, $p = 0.4$) and mutation load (21 vs. 4 events, $p = 0.05$). No correlations were seen between ASHM and the type of organ transplanted, immunosuppression, site of PTLD or phenotype. Notably, all three recurrent PTLD acquired additional mutations in at least one gene, compared to the initial sample. Although, not statistically significant, a greater number of patients who died from disease had evidence of ASHM compared to those who died of other causes or are alive (4/6, 66.7% vs. 2/10, 20%, $p = 0.1$). The former also had a higher number of mutations (20 vs. 5 events, $p = 0.07$), with similar mean follow up durations for the two groups (31.5 vs. 32.7 months, $p = 0.96$).

Gene expression profile analysis

To investigate whether PTLD are characterized by a distinct gene expression signature, we compared gene expression profiles of 12 PTLD with 39 B-NHL samples representative of lymphomas of GC/post-GC derivation. Unsupervised hierarchical clustering showed that, with the exception of the M-PTLD with GC phenotype and the IM-like lesion, all PTLD segregated as a separate group (Figure 1). Additionally, PTLD expression profiles were also different from CLL, MCL [23,27] and marginal zone B-cell lymphomas (GB, unpublished data). Thus, non-GC PTLD appear to represent a distinct type of B-NHL.

Supervised analysis, performed to identify genes differentially expressed between PTLD and normal or transformed B-cells, detected four genes whose expression levels were significantly higher in PTLD (*PRDM1/BLIMP-1*, *XBP-1*, *IFITM3* and *PCMT1*) and only one gene (*C19ORF6*), of unknown function, which was expressed at lower levels (Figure 2).

Both unsupervised and supervised analyses failed to distinguish P-PTLD from non-GC M-PTLD or EBV+ PTLD ($n = 8$) from EBV− PTLD ($n = 4$) (Figure 1 and data not shown).

Finally, in an attempt to better define the cell of origin of PTLD, we applied a classification procedure that measures the relatedness of PTLD gene expression profiles to those of normal B-cell subsets [27]. PTLD expression profiles were first compared to the gene expression signature that distinguishes GC (centroblasts and centrocytes) from non-GC (naïve and memory) B-cells. This analysis showed that PTLD are significantly more similar to non-GC B-cells (Figure 3A, E). On comparing PTLD with naïve and memory B-cells, PTLD appeared more related to memory B-cells (Figure 3B, E). Lastly, we evaluated the relationship of PTLD to memory B-cells versus EBV-immortalized lymphoblastoid cell lines (LCL), representative of activated B-cells, or multiple myeloma (MM) cell lines, representative of terminally differentiated plasma cells. In both analyses, the PTLD expression profile appeared significantly more similar to that of LCLs (Figure 3C–E).

Discussion

The present study was aimed at elucidating the molecular histogenesis of PTLD by performing a comprehensive immunophenotypic, genetic and genome-wide expression analysis on a panel of PTLD representative of the polymorphic and monomorphic subtypes. Our findings

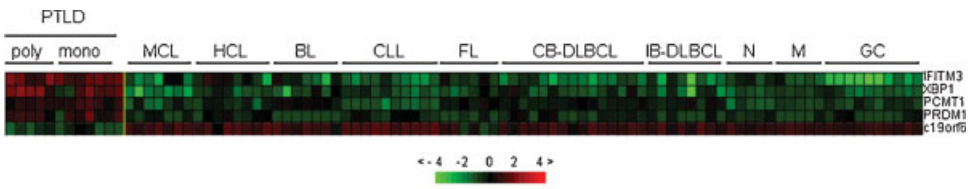

Probe Set ID	Gene Symbol	Gene Title
41745_at	IFITM3	interferon induced transmembrane protein 3 (1-8U)
39755_at	XBP1	X-box binding protein 1
37737_at	PCMT1	protein-L-isoaspartate (D-aspartate) O-methyltransferase
31779_s_at	PRDM1	PR domain containing 1, with ZNF domain
41291_at	C19orf6	chromosome 19 open reading frame 6

Figure 2. Supervised analysis to identify differentially expressed genes between PTLD (5 polymorphic, 6 monomorphic and 1 IM-like lesion) and a representative panel of normal and neoplastic B-cells, which consists of 7 mantle cell lymphomas (MCL), 8 hairy cell leukaemias (HCL), 7 Burkitt lymphomas (BL), 10 chronic lymphocytic leukaemias (CLL), 6 follicular lymphomas (FL), 23 DLBCL (15 centroblastic—CB-DLBCL, 8 immunoblastic—IB-DLBCL), naïve and memory B-cells (5 each), and 10 germinal centre B-cells. In the matrix, columns represent samples and rows correspond to genes. The scale bar provides visualization of difference in the z-scores (expression difference/standard deviation) relative to the mean. Genes are ranked based on the z-score (mean expression difference of the respective gene between phenotype and control group/standard deviation). Affymetrix probe set ID, gene symbol and title is provided for the differentially expressed genes

DOI: 10.1002/hon

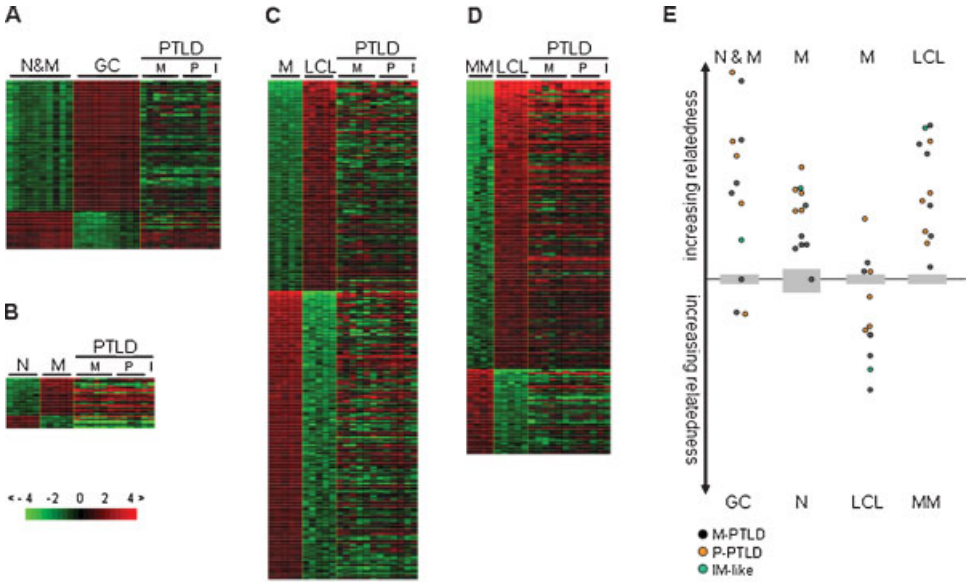

Figure 3. Supervised analysis to identify differentially expressed genes between two groups of samples: (A) naïve and memory B-cells (N&M) compared to germinal centre (GC) B-cells; (B) naïve B-cells compared to memory B-cells; (C) EBV-transformed lymphoblastoid cell lines (LCL) compared to memory B-cells; (D) multiple myeloma cell lines (MM) compared to LCL. Expression of the selected genes investigated in PTLD is depicted on the right side of each matrix. In the matrices, each row represents a gene and each column represents a sample. Genes are ranked according to the z-score (mean expression difference of the gene between the phenotype group and the control group/standard deviation). The scale bar represents differences in the z-score relative to the mean. (E) Cell type classification to measure the relatedness of PTLD with the investigated populations. The grey area marks the 95% of confidence: *p*-value decreases with increasing distance from the *X*-axis

show that (1) non-GC PTLD are a homogeneous group of lymphoproliferations distinct from other B-NHL, as assessed by gene expression profiling; (2) the gene expression signature of non-GC PTLD is related to that of activated memory B-cells; (3) PTLD progression is associated with accrual of genetic lesions and (4) BCR abnormalities in PTLD have a multifactorial etiology.

Non-GC PTLD are distinct from other B-NHL subtypes

The relationship of PTLD to B-NHL of immunocompetent hosts is unknown. In fact, B-cell M-PTLD are morphologically indistinguishable from DLBCL (or BL), while P-PTLD do not resemble any currently recognizable type of B-NHL. Our comparative gene expression analysis of PTLD with other types of B-NHL demonstrates that non-GC PTLD have a homogeneous expression profile that differs from that of other types of B-NHL, including DLBCL (Figure 1). The histogenesis of GC PTLD could not be addressed by our study; however, the single GC PTLD in our series clustered with other GC type B-NHL of immunocompetent hosts. The observation that, on supervised analysis, PTLD only showed differential upregulation of transcription factors associated with plasma cell differentiation [33] suggests similarities with activated B-cell like DLBCL [34]. The DLBCL used in this study were not classified into cell-of-origin-based subgroups using a gene expression signature [34]. However, our unsupervised analysis included immunoblastic lymphomas, a subset of which are known to have phenotypes analogous to activated B-cell like DLBCL [35]. Thus, the unique clustering of PTLD most likely reflects distinct biologic features of these types of B-NHL.

PTLD also differ from DLBCL of immunocompetent hosts with regard to associated genetic lesions, specifically ASHM. The frequency of mutated post-transplant DLBCL was lower compared to DLBCL of immunocompetent hosts for all non-Ig genes except *c-MYC* and *CIITA* [6] (L. P. unpublished data), and all genes showed a lower average mutation frequency compared to *de novo* DLBCL [6]. Furthermore, no *PIM1* mutations were observed, similar to an earlier report [5]. Overall, our data, in conjunction with previous findings in PTLD and HIV-associated B-NHL, suggest that immunosuppression-related lymphomas have lower frequencies of ASHM [5,36].

Non-GC PTLD are related to activated memory B-cells

Virtually, all clonal PTLD in our study appeared to arise from antigen selected B-cells and the majority (74%) had non-GC phenotypes. These data extend the results of prior studies indicating derivation of PTLD from GC experienced B-cells, which have the phenotype of pre-terminally differentiated B-cells, that is BCL6+/−/MUM1+/CD138− [2,7,8]. Of note, one P-PTLD lacked IgV_H mutations, but had *BCL6* mutations. The latter, in the absence of IgV_H mutations, have previously been reported in other types of B-NHL, including PTLD [2]. This could reflect the stochastic nature of mutations targeting the two different loci by SHM [37], suggesting GC transit in the absence of Ig mutations.

DOI: 10.1002/hon

When compared to normal B-cell subsets, gene expression profiles of the non-GC PTLD were most similar to those of resting memory B-cells (Figure 3B, E). However, a comparison between PTLD, resting memory B-cells and LCLs showed a closer similarity of PTLD with LCLs (Figure 3C, E), which represent activated B-cells[38] and have expression profiles similar to IgM-activated B-cells [39]. Our findings, thus, support the hypothesis that non-GC PTLD, both EBV+ and EBV−, may derive from an activated memory B-cell. The suggestion that some PTLD are derived from memory B-cells was made by Timms *et al*. [8] based on the presence of Ig mutations with evidence of antigen selection. Previous studies had also pointed to similarities in the phenotypes and latent viral gene expression profiles between PTLD and LCLs or tumours developing in SCID mice inoculated with EBV infected human lymphocytes [40,41]. Since memory B-cells serve as reservoirs of latent EBV infection [42], it is conceivable that, in the setting of deregulated immune surveillance, activation or acquisition of growth advantage of cells within this compartment could result in a PTLD.

Relationships between different types of PTLD

Our results show that the gene expression programs of P-PTLD and non-GC M-PTLD are indistinguishable, as both unsupervised and supervised gene expression analyse could not segregate them into two distinct groups. This finding was somehow unexpected given the differences in morphology, cellular composition, and genetic abnormalities that characterize these two types of PTLD [1,3]. This is also the case with ASHM, which appears to be rare in P-PTLD but occurs in the majority of M-PTLD, as shown by our and a previous study [5]. One possible explanation for the inability of gene expression analysis to separate P-PTLD and M-PTLD is the existence of heterogeneity within one or both subtypes investigated. The observation that distinct or different combinations of genes are targeted by ASHM in different M-PTLD, suggests biologic differences among cases. However, an effect of subtle qualitative differences in cellular composition cannot be entirely excluded. If these assumptions are true, then a significantly larger survey will be required to identify distinct subsets within these two morphologic categories.

It has been hypothesized that PTLD progress along a continuum from polyclonal early lesions to monocloclonal M-PTLD [1,43]. The identification of cytogenetic aberrations common to both P-PTLD and M-PTLD supports this view [4]. However, a direct relationship between P-PTLD and M-PTLD has not been conclusively established. Only a few studies have evaluated clonal relatedness of PTLD, and clonal identity has been confirmed only in a handful of recurrent M-PTLD and one recurrent P-PTLD [1,43–45]. Our analysis provides evidence of a clonal relationship between a P-PTLD and a metachronous non-GC M-PTLD for the first time, supporting a precursor–product relationship between some P-PTLD and M-PTLD.

In our study, EBV+ and EBV− PTLD did not show significant differences in gene expression profiles, suggesting a similar histogenesis of these PTLD subtypes. This result is in contrast to a recent study by Craig *et al.* who described differentially expressed genes, including EBV regulated transcripts, among EBV+ and EBV− M-PTLD [46]. The differing results may be due to only a few cases analysed in both studies, differences in the types of cases evaluated or methodological differences in the biostatistical analyses. We performed a stringent analysis to identify only consistent differences among EBV+ and EBV− PTLD, using both P-PTLD and M-PTLD. The gene expression differences among EBV+ and EBV− cases identified by Craig *et al.* require validation by generating a classifier and testing them in an independent panel of cases, to demonstrate robustness of the expression differences. Clearly, larger series of PTLD of similar phenotypes need to be analysed to determine differences or similarities between EBV+ and EBV− PTLD.

It also remains to be determined whether EBV+ and EBV− PTLD share aberrations of signalling cascades, cell cycle regulators or proto-oncogenes, as has been suggested for classical Hodgkin lymphoma (cHL) [47]. The observation of an EBER+ M-PTLD that recurred as a clonally related EBER− M-PTLD, raises the possibility that certain EBV− PTLD may result from 'hit and run' oncogenesis [48], similar to EBV− sporadic BL and cHL [49,50]. A comprehensive survey to detect viral genomes in EBV− PTLD is required to definitively exclude a role of EBV or other viruses in the pathogenesis of such lymphoproliferations.

Disease progression is associated with accrual of genetic lesions

We could document accumulation of additional mutations by the neoplastic clone in three recurrent PTLD (including an M-PTLD representing progression of a prior P-PTLD). These findings might reflect clonal heterogeneity at inception, with survival of clones harbouring additional advantageous mutations, or may result from ongoing ASHM activity, as has been described for HIV-related B-NHL [36]. The correlation between presence of ASHM and AID expression by neoplastic cells makes the latter tenable. Our data, in conjunction with prior studies, suggest that progression of PTLD is associated with accrual of genetic lesions [1,4,5]. We speculate that a higher mutation frequency of non-Ig genes may connote recalcitrant disease, similar to observations in B-NHL of immunocompetent hosts [51]. However, larger series of recurrent PTLD need to be studied to evaluate the impact of ASHM on disease progression and prognosis.

B-cell receptor abnormalities in PTLD have a multifactorial etiology

Our analysis showed absent or reduced sIg_L expression by flow cytometry in 32% of PTLD. While similar to earlier studies [52,53], a more recent report described a higher frequency of sIg_L loss (≈76%) based on IHC staining [54]. These discrepancies may be due to lower sensitivity of IHC-based methods compared to flow cytometry, as has been reported for other B-NHL [55].

DOI: 10.1002/hon

Crippling IgV_H gene mutations accounted for loss of sIg_L in only half of sIg_L- PTLD. In contrast to observations in cHL [56], no loss of OCT2 expression was seen in our sIg_L- PTLD, in accordance with a recent report [57]. Absent PU.1 expression was seen in 4/6 (67%) sIg_L- PTLD, confirming the observations of a recent study [57]. This may be due to defective PU.1 expression, as proposed [57], or it may reflect activation of a plasma cell differentiation program [58]. Consistent with the latter hypothesis, three of our sIg_L- PTLD showed phenotypic evidence of transition to plasma cells, as evidenced by CD20 downregulation, cytoplasmic light chain expression, BLIMP-1 protein expression and/or CD43 expression (data not shown).

Capello *et al*. recently reported crippling mutations in Ig_L genes [54]. Since we did not analyse mutations in Ig_L genes, it is unclear whether cytoplasmic light chain expression, as observed in two of our sIg_H+ sIg_L- PTLD, is due to Ig_L gene mutations or other aberrations. Expression of sIg_H in the absence of sIg_L has been reported in LCLs and certain types of B-NHL [59–61]. The etiology of this phenomenon appears multifactorial, some of the proposed mechanisms include truncations in the V_H region secondary to abnormal splicing [59], post-translational defects [62] and abnormal intracellular transport [63].

Irrespective of the mechanism of BCR loss, immunosuppression may allow the survival of BCR-deficient B-cells, as detected in recipients of solid organ allografts [64]. In EBV+ PTLD, the virus itself may rescue B-cell clones, which lack evidence of antigen selection or have crippling Ig mutations [2,7,8], a hypothesis supported by recent *in vitro* experiments [11]. However, the finding of sIg− EBV− PTLD by us and others [54] suggests that as yet unknown molecular alterations of the neoplastic cells may allow survival of EBV− BCR-deficient lymphocytes.

In summary, our findings indicate that non-GC PTLD are distinct from other B-NHL and appear closely related to activated memory B-cells. It is likely that distinct morphologic categories of PTLD are biologically heterogeneous. Further studies are required to explore the relationship of PTLD with other types of immunodeficiency-associated B-NHL.

Acknowledgements

GB would like to thank Dr Glauco Frizzera, formerly at Weill Cornell Medical Center, for morphologic review of PTLD and providing impetus for this study, and Dr Michael L. Shelanski for providing intramural funding.

References

1. Knowles DM, Cesarman E, Chadburn A, *et al*. Correlative morphologic and molecular genetic analysis demonstrates three distinct categories of posttransplantation lymphoproliferative disorders. *Blood* 1995; **85**(2): 552–565.
2. Capello D, Cerri M, Muti G, *et al*. Molecular histogenesis of posttransplantation lymphoproliferative disorders. *Blood* 2003; **102**(10): 3775–3785.
3. Cesarman E, Chadburn A, Liu YF, Migliazza A, Dalla-Favera R, Knowles DM. BCL-6 gene mutations in posttransplantation lymphoproliferative disorders predict response to therapy and clinical outcome. *Blood* 1998; **92**(7): 2294–2302.
4. Vakiani E, Nandula SV, Subramaniyam S, *et al*. Cytogenetic analysis of B-cell posttransplant lymphoproliferations validates the World Health Organization classification and suggests inclusion of florid follicular hyperplasia as a precursor lesion. *Hum Pathol* 2007; **38**(2): 315–325.
5. Cerri M, Capello D, Muti G, *et al*. Aberrant somatic hypermutation in post-transplant lymphoproliferative disorders. *Br J Haematol* 2004; **127**(3): 362–364.
6. Pasqualucci L, Neumeister P, Goossens T, *et al*. Hypermutation of multiple proto-oncogenes in B-cell diffuse large-cell lymphomas. *Nature* 2001; **412**(6844): 341–346.
7. Brauninger A, Spieker T, Mottok A, Baur AS, Kuppers R, Hansmann ML. Epstein-Barr virus (EBV)-positive lymphoproliferations in post-transplant patients show immunoglobulin V gene mutation patterns suggesting interference of EBV with normal B cell differentiation processes. *Eur J Immunol* 2003; **33**(6): 1593–1602.
8. Timms JM, Bell A, Flavell JR, *et al*. Target cells of Epstein-Barr-virus (EBV)-positive post-transplant lymphoproliferative disease: similarities to EBV-positive Hodgkin's lymphoma. *Lancet* 2003; **361**(9353): 217–223.
9. Nelson BP, Nalesnik MA, Bahler DW, Locker J, Fung JJ, Swerdlow SH. Epstein-Barr virus-negative post-transplant lymphoproliferative disorders: a distinct entity? *Am J Surg Pathol* 2000; **24**(3): 375–385.
10. Dotti G, Fiocchi R, Motta T, *et al*. Epstein-Barr virus-negative lymphoproliferate disorders in long-term survivors after heart, kidney, and liver transplant. *Transplantation* 2000; **69**(5): 827–833.
11. Bechtel D, Kurth J, Unkel C, Kuppers R. Transformation of BCR-deficient germinal-center B cells by EBV supports a major role of the virus in the pathogenesis of Hodgkin and posttransplantation lymphomas. *Blood* 2005; **106**(13): 4345–4350.
12. Harris N, Swerdlow S, Frizzera G, Knowles D. Post-transplant lymphoproliferative disorders. In *Tumours of Haematopoietic and Lymphoid Tissues*, Jaffe E, Harris N, Vardiman J (eds). International Agency for Research on Cancer: Lyon, 2001; 264–269.
13. Cattoretti G, Buttner M, Shaknovich R, Kremmer E, Alobeid B, Niedobitek G. Nuclear and cytoplasmic AID in extrafollicular and germinal center B cells. *Blood* 2006; **107**(10): 3967–3975.
14. Cattoretti G, Angelin-Duclos C, Shaknovich R, Zhou H, Wang D, Alobeid B. PRDM1/Blimp-1 is expressed in human B-lymphocytes committed to the plasma cell lineage. *J Pathol* 2005; **206**(1): 76–86.
15. Fais F, Gaidano G, Capello D, *et al*. Immunoglobulin V region gene use and structure suggest antigen selection in AIDS-related primary effusion lymphomas. *Leukemia* 1999; **13**(7): 1093–1099.
16. Kuppers R, Rajewsky K, Hansmann ML. Diffuse large cell lymphomas are derived from mature B cells carrying V region genes with a high load of somatic mutation and evidence of selection for antibody expression. *Eur J Immunol* 1997; **27**(6): 1398–1405.
17. Pasqualucci L, Migliazza A, Fracchiolla N, *et al*. BCL-6 mutations in normal germinal center B cells: evidence of somatic hypermutation acting outside Ig loci. *Proc Natl Acad Sci USA* 1998; **95**(20): 11816–11821.
18. Sioutos N, Bagg A, Michaud GY, *et al*. Polymerase chain reaction versus Southern blot hybridization. Detection of immunoglobulin heavy-chain gene rearrangements. *Diagn Mol Pathol* 1995; **4**(1): 8–13.
19. Lossos IS, Tibshirani R, Narasimhan B, Levy R. The inference of antigen selection on Ig genes. *J Immunol* 2000; **165**(9): 5122–5126.
20. Klein U, Goossens T, Fischer M, *et al*. Somatic hypermutation in normal and transformed human B cells. *Immunol Rev* 1998; **162**: 261–280.
21. Migliazza A, Martinotti S, Chen W, *et al*. Frequent somatic hypermutation of the 5′ noncoding region of the BCL6 gene in B-cell lymphoma. *Proc Natl Acad Sci USA* 1995; **92**(26): 12520–12524.

22. Basso K, Klein U, Niu H, *et al*. Tracking CD40 signaling during germinal center development. *Blood* 2004; **104**(13): 4088–4096.
23. Basso K, Liso A, Tiacci E, *et al*. Gene expression profiling of hairy cell leukemia reveals a phenotype related to memory B cells with altered expression of chemokine and adhesion receptors. *J Exp Med* 2004; **199**(1): 59–68.
24. Klein U, Gloghini A, Gaidano G, *et al*. Gene expression profile analysis of AIDS-related primary effusion lymphoma (PEL) suggests a plasmablastic derivation and identifies PEL-specific transcripts. *Blood* 2003; **101**(10): 4115–4121.
25. Eisen MB, Spellman PT, Brown PO, Botstein D. Cluster analysis and display of genome-wide expression patterns. *Proc Natl Acad Sci USA* 1998; **95**(25): 14863–14868.
26. Lepre J, Rice JJ, Tu Y, Stolovitzky G. Genes@Work: an efficient algorithm for pattern discovery and multivariate feature selection in gene expression data. *Bioinformatics* 2004; **20**(7): 1033–1044.
27. Klein U, Tu Y, Stolovitzky GA, *et al*. Gene expression profiling of B cell chronic lymphocytic leukemia reveals a homogeneous phenotype related to memory B cells. *J Exp Med* 2001; **194**(11): 1625–1638.
28. Hans CP, Weisenburger DD, Greiner TC, *et al*. Confirmation of the molecular classification of diffuse large B-cell lymphoma by immunohistochemistry using a tissue microarray. *Blood* 2004; **103**(1): 275–282.
29. Torlakovic E, Malecka A, Myklebust JH, *et al*. PU.1 protein expression has a positive linear association with protein expression of germinal centre B cell genes including BCL-6, CD10, CD20 and CD22: identification of PU.1 putative binding sites in the BCL-6 promotor. *J Pathol* 2005; **206**(3): 312–319.
30. Rimsza LM, Roberts RA, Miller TP, *et al*. Loss of MHC class II gene and protein expression in diffuse large B-cell lymphoma is related to decreased tumor immunosurveillance and poor patient survival regardless of other prognostic factors: a follow-up study from the Leukemia and Lymphoma Molecular Profiling Project. *Blood* 2004; **103**(11): 4251–4258.
31. Muramatsu M, Kinoshita K, Fagarasan S, Yamada S, Shinkai Y, Honjo T. Class switch recombination and hypermutation require activation-induced cytidine deaminase (AID), a potential RNA editing enzyme. *Cell* 2000; **102**(5): 553–563.
32. Shaknovich R, Basso K, Bhagat G, *et al*. Identification of rare Epstein-Barr virus infected memory B cells and plasma cells in non-monomorphic post-transplant lymphoproliferative disorders and the signature of viral signaling. *Haematologica* 2006; **91**(10): 1313–1320.
33. Shapiro-Shelef M, Calame K. Plasma cell differentiation and multiple myeloma. *Curr Opin Immunol* 2004; **16**(2): 226–234.
34. Staudt LM, Dave S. The biology of human lymphoid malignancies revealed by gene expression profiling. *Adv Immunol* 2005; **87**: 163–208.
35. Carbone A, Gloghini A, Larocca LM, *et al*. Expression profile of MUM1/IRF4, BCL-6, and CD138/syndecan-1 defines novel histogenetic subsets of human immunodeficiency virus-related lymphomas. *Blood* 2001; **97**(3): 744–751.
36. Gaidano G, Pasqualucci L, Capello D, *et al*. Aberrant somatic hypermutation in multiple subtypes of AIDS-associated non-Hodgkin lymphoma. *Blood* 2003; **102**(5): 1833–1841.
37. Pasqualucci L, Neri A, Baldini L, Dalla-Favera R, Migliazza A. BCL-6 mutations are associated with immunoglobulin variable heavy chain mutations in B-cell chronic lymphocytic leukemia. *Cancer Res* 2000; **60**(20): 5644–5648.
38. Young LS, Rickinson AB. Epstein-Barr virus: 40 years on. *Nat Rev Cancer* 2004; **4**(10): 757–768.
39. Cahir-McFarland ED, Carter K, Rosenwald A, *et al*. Role of NF-kappa B in cell survival and transcription of latent membrane protein 1-expressing or Epstein-Barr virus latency III-infected cells. *J Virol* 2004; **78**(8): 4108–4119.
40. Rowe M, Young LS, Crocker J, Stokes H, Henderson S, Rickinson AB. Epstein-Barr virus (EBV)-associated lymphoproliferative disease in the SCID mouse model: implications for the pathogenesis of EBV-positive lymphomas in man. *J Exp Med* 1991; **173**(1): 147–158.
41. Thomas JA, Hotchin NA, Allday MJ, *et al*. Immunohistology of Epstein-Barr virus-associated antigens in B cell disorders from immunocompromised individuals. *Transplantation* 1990; **49**(5): 944–953.
42. Babcock GJ, Decker LL, Volk M, Thorley-Lawson DA. EBV persistence in memory B cells in vivo. *Immunity* 1998; **9**(3): 395–404.
43. Nalesnik MA, Jaffe R, Starzl TE, *et al*. The pathology of posttransplant lymphoproliferative disorders occurring in the setting of cyclosporine A-prednisone immunosuppression. *Am J Pathol* 1988; **133**(1): 173–192.
44. Wu TT, Swerdlow SH, Locker J, *et al*. Recurrent Epstein-Barr virus-associated lesions in organ transplant recipients. *Hum Pathol* 1996; **27**(2): 157–164.
45. Kaplan MA, Ferry JA, Harris NL, Jacobson JO. Clonal analysis of posttransplant lymphoproliferative disorders, using both episomal Epstein-Barr virus and immunoglobulin genes as markers. *Am J Clin Pathol* 1994; **101**(5): 590–596.
46. Craig FE, Johnson LR, Harvey SA, *et al*. Gene expression profiling of Epstein-Barr virus-positive and -negative monomorphic B-cell posttransplant lymphoproliferative disorders. *Diagn Mol Pathol* 2007; **16**(3): 158–168.
47. Knecht H, Berger C, McQuain C, *et al*. Latent membrane protein 1 associated signaling pathways are important in tumor cells of Epstein-Barr virus negative Hodgkin's disease. *Oncogene* 1999; **18**(50): 7161–7167.
48. Ambinder RF. Gammaherpesviruses and ''Hit-and-Run'' oncogenesis. *Am J Pathol* 2000; **156**(1): 1–3.
49. Gan YJ, Razzouk BI, Su T, Sixbey JW. A defective, rearranged Epstein-Barr virus genome in EBER-negative and EBER-positive Hodgkin's disease. *Am J Pathol* 2002; **160**(3): 781–786.
50. Razzouk BI, Srinivas S, Sample CE, Singh V, Sixbey JW. Epstein-Barr Virus DNA recombination and loss in sporadic Burkitt's lymphoma. *J Infect Dis* 1996; **173**(3): 529–535.
51. Rossi D, Berra E, Cerri M, *et al*. Aberrant somatic hypermutation in transformation of follicular lymphoma and chronic lymphocytic leukemia to diffuse large B-cell lymphoma. *Haematologica* 2006; **91**(10): 1405–1409.
52. Dunphy CH, Gardner LJ, Grosso LE, Evans HL. Flow cytometric immunophenotyping in posttransplant lymphoproliferative disorders. *Am J Clin Pathol* 2002; **117**(1): 24–28.
53. Kaleem Z, Hassan A, Pathan MH, White G. Flow cytometric evaluation of posttransplant B-cell lymphoproliferative disorders. *Arch Pathol Lab Med* 2004; **128**(2): 181–186.
54. Capello D, Cerri M, Muti G, *et al*. Analysis of immunoglobulin heavy and light chain variable genes in post-transplant lymphoproliferative disorders. *Hematol Oncol* 2006; **24**(4): 212–219.
55. Li S, Eshleman JR, Borowitz MJ. Lack of surface immunoglobulin light chain expression by flow cytometric immunophenotyping can help diagnose peripheral B-cell lymphoma. *Am J Clin Pathol* 2002; **118**(2): 229–234.
56. Stein H, Marafioti T, Foss HD, *et al*. Down-regulation of BOB.1/OBF.1 and Oct2 in classical Hodgkin disease but not in lymphocyte predominant Hodgkin disease correlates with immunoglobulin transcription. *Blood* 2001; **97**(2): 496–501.
57. Lucioni M, Capello D, Riboni R, *et al*. B-cell posttransplant lymphoproliferative disorders in heart and/or lungs recipients: clinical and molecular-histogenetic study of 17 cases from a single institution. *Transplantation* 2006; **82**(8): 1013–1023.
58. Pettersson M, Sundstrom C, Nilsson K, Larsson LG. The hematopoietic transcription factor PU.1 is downregulated in human multiple myeloma cell lines. *Blood* 1995; **86**(7): 2747–2753.
59. Cogne M, Silvain C, Khamlichi AA, Preud'homme JL. Structurally abnormal immunoglobulins in human immunoproliferative disorders. *Blood* 1992; **79**(9): 2181–2195.
60. Hendershot L, Levitt D. Analysis of surface mu-chain expression in human lymphoblastoid cell lines that do not produce light chains. *J Immunol* 1984; **132**(1): 502–509.
61. Kaleem Z, Zehnbauer BA, White G, Zutter MM. Lack of expression of surface immunoglobulin light chains in B-cell non-Hodgkin lymphomas. *Am J Clin Pathol* 2000; **113**(3): 399–405.

DOI: 10.1002/hon

62. Vuillier F, Dumas G, Magnac C, *et al*. Lower levels of surface B-cell-receptor expression in chronic lymphocytic leukemia are associated with glycosylation and folding defects of the mu and CD79a chains. *Blood* 2005; **105**(7): 2933–2940.
63. Lee BS, Alvarez X, Ishido S, Lackner AA, Jung JU. Inhibition of intracellular transport of B cell antigen receptor complexes by Kaposi's sarcoma-associated herpesvirusK1. *J Exp Med* 2000; **192**(1): 11–21.
64. Schauer E, Webber S, Green M, Rowe D. Surface immunoglobulin-deficient Epstein-Barr virus-infected B cells in the peripheral blood of pediatric solid-organ transplant recipients. *J Clin Microbiol* 2004; **42**(12): 5802–5810.

DOI: 10.1002/hon